Turkish Journal of Electrical Engineering & Computer Sciences

http://journals.tubitak.gov.tr/elektrik/

Research Article

Turk J Elec Eng & Comp Sci
(2019) 27: 3567 – 3581

doi:10.3906/elk-1811-59

An improved imperialist competitive algorithm for global optimization

Ting YOU[1,2], **Yueli HU**[1,3,*], **Peijiang LI**[2], **Yinggan TANG**[4]

[1]School of Mechatronics Engineering and Automation, Shanghai University, Shanghai, P.R. China
[2]School of Electrical and Information Engineering, QuZhou College, QuZhou, Zhejiang, P.R. China
[3]Shanghai Key Laboratory of Power Station Automation Technology, Shanghai University, Shanghai, P.R. China
[4]Institute of Electrical Engineering, Yanshan University, Qinhuangdao, Hebei, P.R. China

Received: 09.11.2018 • **Accepted/Published Online:** 27.05.2019 • **Final Version:** 18.09.2019

Abstract: The imperialist competitive algorithm (ICA), inspired by sociopolitical behavior in the real world, is a new optimization algorithm. The ICA shows great potential to solve complex optimization problems. In order to improve the ICA's exploration ability and speed up its convergence, two improved schemes are proposed in this paper. The first scheme presents a new possession probability in the imperialistic competition phase. Inspired by geopolitics, not only the power of the empire but also the distance between the imperialists are taken into account in calculating the new possession probability. The second scheme introduces the wavelet mutation operator into the original ICA so as to improve its exploration ability. The improved ICAs (IICAs) are tested on several benchmark functions and then used to design the optimum parameters of tuned mass damper and tune the parameters of a fractional order PID controller of an automatic voltage regulator (AVR) system. Results show that the IICAs outperform the original ICA in terms of solution quality and convergence speed.

Key words: Global optimization, imperialist competitive algorithm, wavelet mutation, geopolitics, tuned mass damper, automatic voltage regulator

1. Introduction

Frequently, optimization is encountered in various scientific and engineering fields and plays a very important role in solving problems. In the past decades, classic optimization algorithms underwent extensive development. They are based on rigorous mathematical inference; however, they impose restricted conditions on the objective function and may easily be trapped in local optimal and converge slowly, which has hampered finding solutions to real-world optimization problems. Recently, evolutionary optimization algorithms, inspired by the biological behavior of social insects or organizations, have been developed to solve various complex optimization problems. Compared with classic optimization techniques, evolutionary algorithms (EAs) impose no restrictions on the objective function and possess the global searching ability. The genetic algorithm (GA) [1], particle swarm optimization (PSO) [2], ant colony optimization (ACO) [3], and artificial bee colony (ABC) [4] are just a few examples. These algorithms show great potential in solving various complex optimization problems in business, industry, engineering, computer science, and other fields.

The imperialist competitive algorithm (ICA) was proposed by Atashpaz-Gargari and Lucas in 2007, inspired by sociopolitical processes of imperialistic competition of human beings in the real world [5]. Since its proposition, the ICA was extensively investigated and widely applied in various domains, such as electrical

*Correspondence: Yuelihu21@163.com

power system optimization [6, 7], neural network training [8], flowshop scheduling [9, 10], data clustering [11], facility layout problem [12], minimal spanning tree problem [12], and so on.

Though the ICA has some advantages such as fast convergence rate and better global minimum achievement, there still are some inefficiencies associated with it [13–15], which were surveyed in [12] in detail. Like other EAs, premature convergence may occur in different situations. To prevent premature phenomena, mutation operators are added to the ICA. In [16], a modified ICA (MICA) was proposed. In MICA, 10 randomly mutated individuals are generated in each iteration, and the best mutated individual replaces the current country if it is better than the current country. Then the best solution found by MICA is further updated by simulated annealing (SA). In [14], a mutation operation, as the mutation in differential evolution (DE), was performed after colonies moved towards the imperialist. In [17], a hybrid ICA with GA was proposed. In the algorithm, the mutation operator in the GA is introduced into the revolution step in the ICA. On the other hand, the exploration capability of the ICA is unsatisfactory. To enhance the exploration capability of the ICA, several modified schemes have been proposed. In [18, 19], a chaotic map was introduced to adjust the angles of colonies' movements toward imperialists. In [13], an adaptive ICA (AICA) was proposed. In AICA, the angles of colonies moving towards imperialists are adapted through an absorption policy that changes dynamically. In [20, 21], the concept of attraction and repulsion between the colony and its imperialists was introduced for searching for better solutions. In [15], a chaotic ICA was suggested, where chaotic maps are used to improve the movement of colonies. A gbest-guided ICA was developed in [22] to improve the exploitation. In [23], a hybrid ICA-PSO algorithm was presented for single-objective and multiobjective problems. In [24], a fuzzy adaptive ICA was proposed, where the deviation parameter is adaptively adjusted using a fuzzy controller.

In this paper, two schemes are proposed to improve the performance of the ICA. The first scheme presents a new possession probability in the imperialistic competition phase. The new possession probability, which is inspired by geopolitics, takes the power of the empire and the distance between the imperialist and the colonies into account. The second scheme introduces the wavelet mutation operator into the original ICA to improve its exploration ability.

The rest of this paper is organized as follows. The basic ICA and the improved schemes for the ICA are given in Section 2. In Section 3, simulation results and discussions are presented. Finally, the conclusions are summarized in Section 4.

2. Improved ICA

2.1. Brief review of ICA

For the sake of argument, the basic process of the ICA is reviewed. More details about the ICA can be found in [5]. The ICA manages a population of individuals, each of them called a country. These countries are classified as imperialists or colonies according to their power. Each imperialist possesses some colonies and they constitute an empire. Empires compete with each other in the evolving process. If an empire fails in the competition, it will lose its colonies, and therefore its power will become weaker and weaker. When it loses its all colonies, the empire collapse. Finally, the ICA converges until only one empire exists. The ICA consists of four steps: initialization, assimilation, competition, and finally convergence. In the initialization stage, the ICA randomly generates a set of countries as follows:

$$country = [p_1, p_2, \cdots, p_{N_{var}}]. \tag{1}$$

The cost of a country is calculated by evaluating the cost function with the variable $(p_1, p_2, \cdots, p_{N_{var}})$, i.e.

$$cost = f(country) = f(p_1, p_2, \cdots, p_{N_{var}}). \tag{2}$$

After this, N_{imp} of the most powerful countries are selected as imperialists and the remaining N_{col} countries will be colonies. The next step after initialization is to form empires by assigning colonies to a certain imperialist according to the imperialist's normalized cost.

After empires' formation, the colonies in an empire move toward the corresponding imperialist to enhance the power of the empire. This process is called assimilation. If one colony reaches a better position than that of the imperialist, the colony becomes a new imperialist and the previous imperialist becomes a colony.

After assimilation, empire competition begins, which leads to an increase in the power of more powerful empires and a decrease in the power of weaker ones. The competition is implemented by just picking some (usually one) of the weakest colonies of the weakest empires and making a competition among all empires to possess these (this) colonies. In the competition, each empire has a chance to possess the colonies according to its total power. The probability of each empire possessing the colonies is defined as:

$$P_{p_n} = \left| \frac{NTC_n}{\sum_{i=1}^{N_{imp}} NTC_i} \right|, \tag{3}$$

where N_{imp} is the number of imperialist countries and NTC_n is the normalized total cost of the nth empire, which is defined as

$$NTC_n = TC_n - \max_i\{TC_i\}, i = 1, 2, \cdots, N_{imp}. \tag{4}$$

In order to divide the mentioned colonies among empires based on the possession probability of them, a vector P is defined as

$$P = \left[P_{p_1}, P_{p_2}, \cdots, P_{p_{imp}}\right]. \tag{5}$$

Then a vector R is created with the same size as vector P:

$$R = \left[r_1, r_2, \cdots, r_{N_{imp}}\right], r_i \sim U(0,1) \tag{6}$$

A vector D is defined as follows:

$$D = P - R. \tag{7}$$

The empire whose relevant index is maximum in D will occupy the weakest colony of the weakest empire. If an empire loses all its colonies, it will collapse. The assimilation and competition process repeats several times until only one empire exists. Then the ICA converges to a state in which all the colonies and imperialists have the same cost.

2.2. Improved ICAs

To enhance the convergence speed and the solution accuracy of the ICA, two improved schemes are proposed in this section.

2.2.1. A new possession probability in imperialistic competition

Imperialistic competition is an important step in the ICA. It provides a chance for each empire to increase its power. In the original ICA, imperialistic competition is mainly based on the power of each empire. The more powerful an empire is, the more likely the empire can possess the colonies. This strategy makes the ICA converge in the early searching stage, which is the so-called premature phenomenon. If the premature phenomenon occurs, the algorithm will lose more chances to improve the solution found so far.

In international politics, geopolitics, a term coined by Rudolf Kjellén at the beginning of the twentieth century, is a famous theory that analyzes and predicts international political behavior and the strategic situation of a state or region. Geopolitics regards the geographical factor as a basic factor affecting or determining the nature of a state or a region. In this light, the closer two countries are, the greater effect one country may impose on the other, and vice versa. Owing to this fact, the distance between empires and the weakest colony is taken into consideration in the imperialistic competition as well as the power of the empire. The closer an empire and the weakest colony, the more likely the empire may possess it. Therefore, the possession probability is modified as follows:

$$P'_{P_n} = \lambda_1 \left| \frac{NTC_n}{\sum_{i=1}^{N_{imp}} NTC_i} \right| + \lambda_2 \left| \frac{Dis_n}{\sum_{i=1}^{N_{imp}} Dis_i} \right|, \tag{8}$$

where Dis_i is the distance between the weakest colony and the ith imperialist, which is defined via a Euclidean metric, and λ_1 and λ_2 are two weights that balance the effect of power and geographic distance in the imperialist competition. Eq. (8) indicates that an empire possesses a colony depending not only on its power but also the distance between the empire and the colony in the competition phase. Consequently, the new possessing probability of Eq. (8) enables an empire to more likely possess the weakest colonies. Thus, it promotes the powerful empire to possess more colonies, and as a consequence, the convergence is sped up. In this way, the exploitation of the ICA is enhanced.

2.2.2. Wavelet mutation

Like other EAs, the stronger the exploration capability, the more likely the algorithm is to find the better solution. To enhance the exploration capability, the mutation operator is an efficient strategy. As mentioned in Section 1, several mutation strategies such as random mutation, GA mutation, differential mutation, Gaussian mutation, and Cauchy mutation have been proposed by researchers.

Most mutation operations are implemented stochastically. An important issue for the mutation operator is to generate a high-quality solution. Apart from the above-mentioned mutation operators, the wavelet mutation (WM) operator was proposed by Ling et al. in [25]. Compared to other mutation operators, the WM operator not only can improve the solution stability but also has fine-tuning ability. On the other hand, WM can generate positive and negative solutions with the same probability. Therefore, the WM is adopted in this paper to enhance the exploration ability.

Let $country_i = [p_{i1}, p_{i2}, \cdots, p_{iN_{var}}]$ be the ith country selected for mutating, and the WM mutated country is

$$\overline{country}_i = country_i(1 + \chi(\cdot)), \tag{9}$$

where $\chi(\cdot)$ is a random variable of obeying a wavelet probability distribution whose density function is described by a wavelet function. In this paper, a Morlet wavelet function is adopted, i.e.

$$\chi(\vartheta) = e^{\frac{-\vartheta^2}{2}} \cos(5\vartheta), \quad -2.5 \leq \vartheta \leq 2.5. \tag{10}$$

Its density function is shown in Figure 1. In each mutation operation, a random vector ϑ is generated in $[-2.5\ 2.5]$, and then we substitute it into Eq. (10) to obtain another random vector χ. Then the random vector χ is added to the country to be mutated. For example, let $P = [2\ 8]$ be a country to be mutated, and let the random vector ϑ be $[1.5736\ 2.0290]$. According to Eq. (10), random vector $\chi = [-0.0041\ \ -0.0960]$. As a result, the country P after mutation is $P' = P + (1 + \chi) = [2.9959\ 8.9040]$.

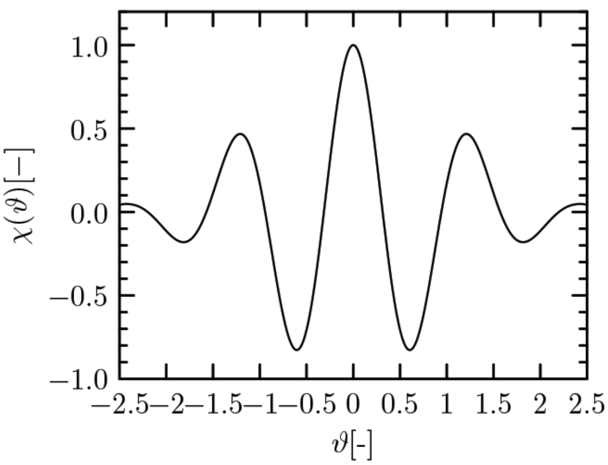

Figure 1. Morlet wavelet density function.

3. Simulation results

To demonstrate their performance, the proposed IICAs are tested on six benchmark functions. The tested algorithms include ICA with new possession probability (IICA-1), ICA with wavelet mutation (IICA-2), and ICA both with new possession probability and wavelet mutation (IICA-3). All the IICAs are compared with the original ICA. In all experiments, the parameters of the ICA and its improved versions are set as follows. The number of countries $N_{country}$ is set to 200, and 8 of the best countries form the imperialists. The other 192 ones are selected as colonies, and λ_1 and λ_2 in Eq. (8) are set to 0.2 and 0.8, respectively, in this paper.

3.1. Benchmark test functions: results and analysis

3.1.1. Benchmark test functions

In this section, six typical benchmark functions are adopted to test the IICAs. The first function is unimodal and the other five functions are multimodal with many local minima, where it is difficult to find the global optimum. These functions and their ranges are listed in Table 1. Function f_1 is a sphere function with only one minimum. Function f_2 is Rastrigin function, which is a complex multimodal problem with a large number of local optima. When attempting to solve the Rastrigin function, algorithms may easily fall into local optima. Functions f_3 and f_4 are Schwefel's functions, whose deepest local optima are far from the global optima. Function f_5 is the Ackley function. It has one narrow global optimum basin and many minor local optima. Function f_6 is the Rosenbrock function.

3.1.2. Results and discussion

In this section, the tested results on the six benchmark test functions are given to show the efficiency of the proposed IICAs. Each algorithm independently runs 30 times for each function. The best, the mean, and the worst cost value, with the standard deviation and convergence rate of the six benchmark functions with dimension 10, are presented in Table 2 and Figure 2.

Table 1. Test functions.

Function name	Expression	Search range	Global minima
Sphere	$f_1(x) = \sum_{i=1}^{n} x_i^2$	$[-100, 100]$	0
Rastrigin	$f_2(x) = \sum_{i=1}^{n}(x_i^2 - 10\cos(2\pi x_i) + 10)$	[-5.12,5.12]	0
Schwefel1.2	$f_3(x) = \sum_{i=1}^{n}(\sum_{j=1}^{i} x_j)^2$	[-100,100]	0
Schwefel2.21	$f_4(x) = \sum_{i=1}^{n} \lvert x_i \rvert$	[-100,100]	0
Ackley	$f_5(x) = -20\exp(-0.2\sqrt{\frac{1}{10}\sum_{i=1}^{n} x_i^2}) - \exp(\sqrt{\frac{1}{10}\sum_{i=1}^{n}\cos(2\pi x_i)}) + 20 + e$	[-32,32]	0
Rosenbrock	$f_6(x) = \sum_{i=1}^{n}[100(x_{i+1} - x_i^2)^2 + (x_i - 1)^2]$	[-30,30]	0

From the results, it can be seen that for function f_1, the results obtained by the three improved ICAs are all better than those of the original ICA. However, IICA-3 is the best among these algorithms. As shown in Figure 2a, the convergence rates of the three improved ICAs have no evident differences from each other; however, they are all faster than the original ICA. This is because this function is unimodal, smooth, and symmetric, making it easy to be solved. For function f_2, which is a multimodal function with many local optima, the improved ICAs all perform better than the original ICA, and IICA-3 performs the best among these reference algorithms. From Figure 2b, the three improved ICAs converge faster than the ICA. Also, the convergence speed of IICA-3 is the fastest. Similar conclusions can be obtained for the remaining four multimodal functions from Figures 2c–2f. Therefore, the improved ICAs show great superiority compared to the original ICA. IICA-3, which adopts new possession probability and has the WM mutation operator, performs the best compared to IICA-1 and IICA-2. The two improved schemes not only improve the solution quality but also increase the convergence speed.

3.1.3. Effects of the weights λ_i

In the first improved scheme, the new possession probability is the weighted sum of the normalized power and distance. To reveal the effect of the two weights on the optimization performance, we test the IICA-1 algorithm with different combinations of weights. The optimization results are statistically listed in Table 3. Figure 3 shows the convergence curve of the IICA-1 for the six benchmark functions. From Table 3 and Figure 3, we can see that the weights in Eq. (8) have little effect on the optimization performance.

3.1.4. Computation efficiency

To show the computation cost of the improved algorithms, Table 4 shows the computation time of each algorithm. It can be seen that the computation costs of the improved ICAs are comparable to each other. In general, the improved algorithms are more computationally efficient than the ICA. That is to say, the improved algorithms do not increase the computation burden.

Table 2. Optimization results of IICA-1, IICA-2, IICA-3, and original ICA through 30 independent runs on six benchmark functions.

Fuctions	Algorithm	Best	Mean	Worst	Standard dev.
f_1	ICA	2.8319e-16	6.9182e-14	6.5782e-13	1.3342e-13
	IICA-1	3.1725e-17	3.3453e-14	2.3830e-13	5.1899e-14
	IICA-2	4.4522e-19	1.2293e-16	1.1527e-15	2.6397e-16
	IICA-3	7.3460e-20	8.5843e-17	5.0433e-16	1.3419e-16
f_2	ICA	1.0534e-11	1.1992e-6	3.3451e-5	6.0052e-6
	IICA-1	1.5987e-14	5.9144e-8	1.7477e-6	3.1457e-7
	IICA-2	3.5527e-15	1.1530e-8	3.3729e-7	6.0498e-8
	IICA-3	0	3.9156e-9	1.0739e-7	1.9250e-8
f_3	ICA	1.4139e-7	4.1120e-5	2.6960e-4	6.4304e-5
	IICA-1	3.9286e-8	1.0438e-5	5.6644e-5	1.3999e-5
	IICA-2	1.0953e-8	2.0209e-6	2.0295e-5	4.0709e-6
	IICA-3	3.5595e-9	5.5918e-7	3.9799e-6	9.7807e-7
f_4	ICA	0.0011	0.0045	0.0180	0.0039
	IICA-1	1.9934e-4	0.0037	0.0136	0.0029
	IICA-2	1.3189e-4	0.0011	0.0106	0.0019
	IICA-3	1.0779e-5	5.1497e-4	0.0019	4.0269e-4
f_5	ICA	1.5252e-8	7.0852e-8	2.3547e-7	5.4622e-8
	IICA-1	7.1000e-9	7.9881e-8	5.5727e-7	1.2140e-7
	IICA-2	1.5518e-10	6.2877e-9	8.6040e-8	1.5528e-8
	IICA-3	2.6611e-11	4.1597e-9	1.8920e-8	5.7006e-9
f_6	ICA	1.6561e-8	5.8113e-5	4.0707e-6	1.0630e-5
	IICA-1	8.2159e-9	9.7549e-6	1.7501e-6	2.6755e-6
	IICA-2	8.0495e-10	2.2039e-5	1.6473e-6	4.5697e-6
	IICA-3	2.9741e-10	6.0600e-7	5.5404e-8	1.2386e-7

3.2. Parameter optimization of tuned mass damper

Tuned mass damper (TMD) is a structural vibration control device invented by Frahm [26]. Nowadays many tall buildings and long-span bridges are equipped with different kinds of TMD systems to attenuate undesirable vibrations caused by strong wind or earthquakes. When a main structure equipped with a TMD system is excited by an external excitation, most of the input energy is absorbed by the TMD system and only a part of the energy is transferred to the main structure system. As a result, the motion of the main structure is controlled and the vibration is attenuated. Usually, a TMD system is made up of a mass, a spring, and a dashpot attached to a main structure. For a TMD system, an important issue is to optimally design its parameters, i.e. mass, damping, and stiffness, such that a satisfactory response of the main structure system can be obtained. Though much effort has been paid, determining the optimal parameters of TMD is still a difficult problem. The commonly used method to optimally design the parameters of TMD is the numerical iteration method. However, this method is sensitive to initial values and easily trapped into local minimum. Recently, many metaheuristic algorithms such as the GA, PSO [27], and harmony search (HS) algorithm [28] have been adopted to design the optimum parameters of TMD systems.

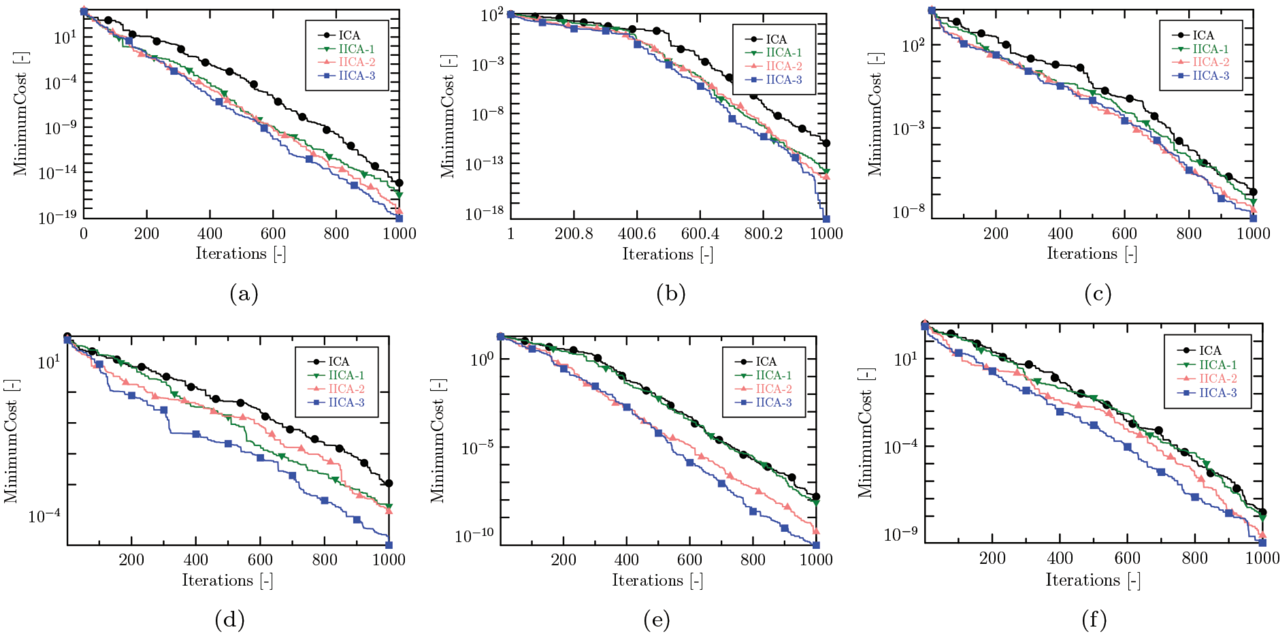

Figure 2. Comparisons between different ICAs for test functions: (a) sphere, (b) Rastrigin, (c) Schwefel1.2, (d) Schwefel12.21, (e) Ackley, (f)Rosenbrock.

Table 3. Optimization results of IICA-1 with different weights (λ_1, λ_2) for six benchmark functions.

Fuctions	$\lambda_1 = 0.8, \lambda_2 = 0.2$	$\lambda_1 = 0.5, \lambda_2 = 0.5$	$\lambda_1 = 0.2, \lambda_2 = 0.8$
f_1	3.1725e-17	1.1697e-16	6.2786e-16
f_2	1.5987e-14	2.4851e-12	4.9081e-12
f_3	3.9286e-8	8.4415e-8	9.7467e-8
f_4	1.9934e-4	4.6074e-4	2.7410e-4
f_5	7.1000e-9	4.0070e-9	6.1764e-9
f_6	8.2159e-9	9.3842e-9	1.6835e-8

In this section, the improved ICAs are used to optimally design the parameters of a TMD system. For the sake of convenience, the main structural system with a TMD system is modeled as a single-degree-of-freedom (SDOF) system and the excitation is an external force applied to the main system, which is shown in Figure 4.

The motion equation of the system is as follows [29]:

$$\begin{bmatrix} m_s & 0 \\ 0 & m_T \end{bmatrix} \begin{Bmatrix} \ddot{x_s} \\ \ddot{x_T} \end{Bmatrix} + \begin{bmatrix} c_s + c_T & -c_T \\ -c_T & c_T \end{bmatrix} \begin{Bmatrix} \dot{x_s} \\ \dot{x_T} \end{Bmatrix} + \begin{bmatrix} k_s + k_T & -k_T \\ -k_T & k_T \end{bmatrix} \begin{Bmatrix} x_s \\ x_T \end{Bmatrix} = \begin{Bmatrix} F \\ 0 \end{Bmatrix}, \tag{11}$$

where x_s is the displacement of the main system relative to the base and x_T is the displacement of TMD relative to the base. m_s, c_s, and k_s are the mass, damping, and stiffness of the main system, respectively, and m_T, c_T, and k_T are the mass, damping, and stiffness of TMD system, respectively. F is the external force applied to the main system, which is assumed to be a Gaussian white noise with constant power spectral S_0. Let $\omega_s = \sqrt{k_s/m_s}$ and $\xi_s = c_s/2\sqrt{k_s m_s}$ be the natural frequency and viscous damping ratio of the main system, respectively. Also, let $\omega_T = \sqrt{k_T/m_T}$ and $\xi_T = c_T/2\sqrt{k_T m_T}$ be the natural frequency and damping

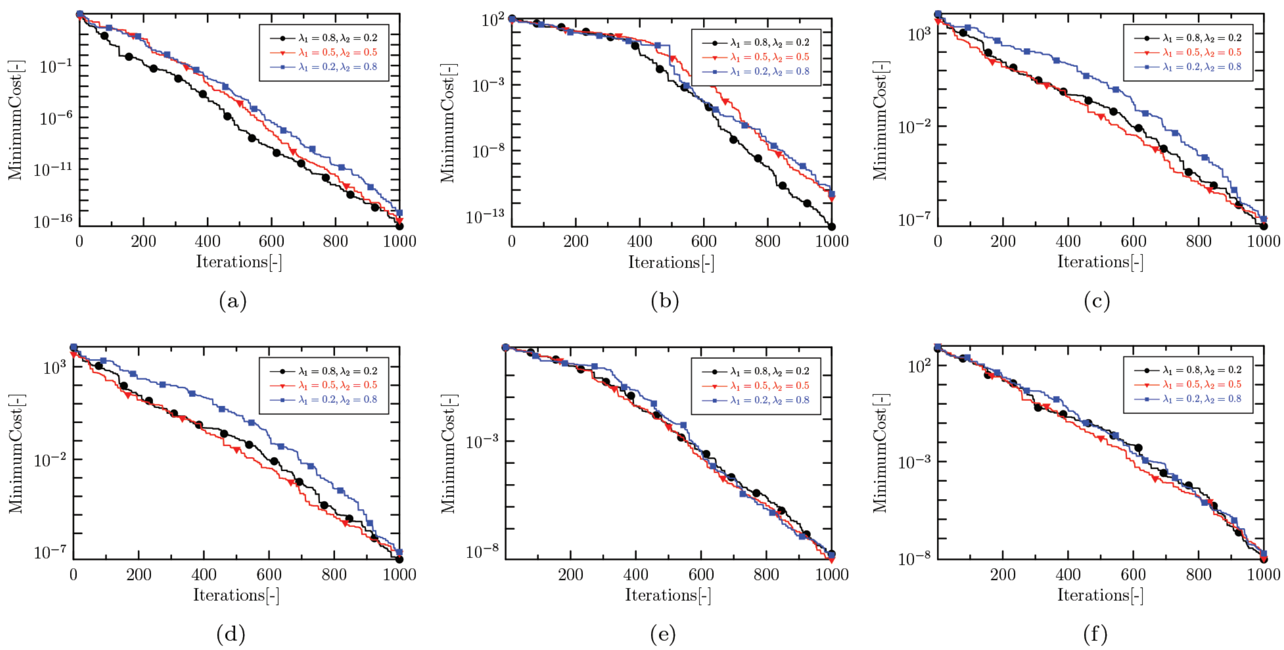

Figure 3. Comparisons between different weighs for test functions: (a) sphere, (b) Rastrigin, (c) Schwefel1.2, (d) Schwefel12.21, (e) Ackley, (f) Rosenbrock.

Table 4. Computation time of each algorithm (s).

	f_1	f_2	f_3	f_4	f_5	f_6
ICA	1.2621	1.6499	0.9603	2.2603	2.2281	1.7617
IICA-1	1.4784	1.5335	1.381	2.099	2.1555	2.3455
IICA-2	0.9336	1.9007	1.0578	2.4555	1.6633	0.9368
IICA-3	0.9016	1.7637	0.9586	2.756	1.5004	0.9276

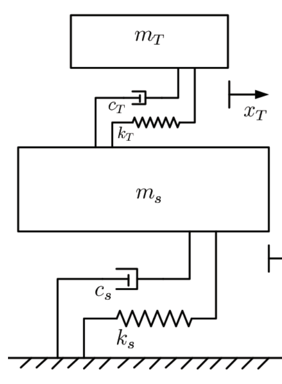

Figure 4. A SODF main system with TMD.

ratio of the TMD system. The mass and tuning frequency ratio of the TMD system are defined as $\eta = m_T/m_s$ and $f = \omega_T/\omega_s$. The mean square displacement response of the main system is

$$\sigma_{x_s}^2 = \int_{-\infty}^{\infty} S_0 |H_{x_s}(\omega)| \mathrm{d}\omega, \tag{12}$$

where

$$H_{x_s}(\omega) = \frac{1}{\Lambda m_s}(-\omega^2 + 2\mathrm{i}\xi_T\omega_T\omega + \omega_T^2), \tag{13}$$

$$\begin{aligned}\Lambda =& \omega^4 - 2\mathrm{i}[\omega_s\xi_s + (1+\eta)\xi_T\omega_T]\omega^3 - [\omega_s^2 + (1+\eta)\omega_T^2 + 4\omega_s\omega_T\xi_s\xi_T]\omega^2 \\ &+ 2\mathrm{i}\omega_s\omega_T[\omega_T\xi_s + \omega_s\xi_T]\omega + \omega_s^2\omega_T^2,\end{aligned} \tag{14}$$

where i is the unit of imaginary number. Let $N = \sigma_{x_s}^2 k_s^2 / 2\pi S_0\omega_s$ be the response quantity of the main system. Substituting Eq. (13) and Eq. (14) into Eq. (12), and after some manipulations, one can obtain the following [29]:

$$N(\eta, \xi_T, f) = \frac{P}{4Q}, \tag{15}$$

where

$$\begin{aligned}P =& \xi_T[1 - f^2(2+\eta) + f^4(1+\eta)^2] + \eta f^3\xi_s + 4f^2\xi_T^3(1+\eta) \\ &+ 4f\xi_T^2\xi_s[1 + f^2(1+\eta)] + 4f^2\xi_T\xi_s^2,\end{aligned} \tag{16}$$

$$\begin{aligned}Q =& \eta f\xi_T^2 + \xi_T\xi_s\{1 - 2f^2 + f^4(1+\eta)^2 + 4f^2\xi_T^2(1+\eta) \\ &+ 4f\xi_T\xi_s[1 + f^2(1+\eta)] + 4f^2\xi_s^2\} + \eta f^3\xi_s^2.\end{aligned} \tag{17}$$

The optimization problem of TMD can be formulated as

$$N^{\mathrm{opt}} = \arg\min_{\eta,\xi_T,f} N(\eta, \xi_T, f), \tag{18}$$

subjected to $\eta > 0, \xi_T > 0, f > 0$. It is observed that for a damped main structural system excited by white noise external force, the optimum response quantity N^{opt} decreases as the mass ratio η increases [27]. Therefore, only the damping and tuning frequency ratio of TMD for specified mass ratio η should be optimized. The ICA and IICAs are used to fulfill this task. The optimum parameters obtained by the ICA and IICAs, PSO [27], and curve fitting [29] are listed in Table 5. It can be seen that the ICA and IICAs obtain the same optimum parameters. The reason for this is that the optimization problem of Eq. (18) has only two optimization variables. Compared to multidimensional optimization problems, the optimization problem of Eq. (18) is relatively simple and the basic ICA can obtain satisfactory optimization results. However, it can be seen that the response quantities of the ICA and IICAs are all smaller than that of PSO and curve fitting for different damping ratios ξ_s. Therefore, it can be concluded that the ICA and IICAs outperform PSO and curve fitting in solving the optimum parameter of TMD. To see this more clearly, Figures 5–7 show the optimum parameters of TMD varying with mass ratio η for $\xi_s = 0.01$, $\xi_s = 0.05$, and $\xi_s = 0.1$. In Figures 5–7, ICAs represent both ICA and IICAs because the optimum parameters of TMD obtained by the ICA and IICAs are the same. Also, the optimum parameters of TMD obtained by PSO and curve fitting are the same, so only the curve for curve fitting is plotted.

Table 5. Optimum TMD parameters obtained through ICAs and PSO and curve fitting for specified mass ratio.

	η	$\xi = 0.01$			$\xi = 0.05$			$\xi = 0.1$		
		ξ_T	f_{opt}	N_{opt}	ξ_T	f_{opt}	N_{opt}	ξ_T	f_{opt}	N_{opt}
ICA	0.01	0.0325	0.9937	4.9549	0.0291	0.9928	1.0114	0.0311	0.9910	0.5726
	0.02	0.0568	0.9864	4.8145	0.0407	0.9865	1.2746	0.0427	0.9842	0.6901
	0.03	0.0756	0.9790	4.3884	0.0505	0.9804	1.4273	0.0516	0.9778	0.7680
	0.05	0.1032	0.9646	3.7101	0.0688	0.9681	1.5786	0.0662	0.9654	0.8675
	0.07	0.1241	0.9508	3.2543	0.0866	0.9556	1.6300	0.0789	0.9535	0.9266
	0.09	0.1414	0.9376	2.9292	0.1037	0.9430	1.6348	0.0908	0.9419	0.9631
	0.1	0.1490	0.9312	2.7986	0.1119	0.9367	1.6277	0.0965	0.9361	0.9757
IICA-1	0.01	0.0322	0.9935	4.9550	0.0291	0.9928	1.0114	0.0311	0.9910	0.5726
	0.02	0.0570	0.9854	4.8145	0.0407	0.9865	1.2746	0.0427	0.9842	0.6901
	0.03	0.0756	0.9790	4.3884	0.0505	0.9804	1.4273	0.0516	0.9778	0.7680
	0.05	0.1032	0.9646	3.7101	0.0688	0.9681	1.5786	0.0662	0.9654	0.8675
	0.07	0.1241	0.9508	3.2543	0.0866	0.9556	1.6300	0.0789	0.9535	0.9266
	0.09	0.1414	0.9376	2.9292	0.1037	0.9430	1.6348	0.0908	0.9419	0.9631
	0.1	0.1490	0.9312	2.7986	0.1119	0.9367	1.6277	0.0965	0.9361	0.9757
IICA-2	0.01	0.0325	0.9937	4.9549	0.0291	0.9928	1.0114	0.0311	0.9910	0.5726
	0.02	0.0568	0.9864	4.8145	0.0407	0.9865	1.2746	0.0427	0.9842	0.6901
	0.03	0.0756	0.9790	4.3884	0.0505	0.9804	1.4273	0.0516	0.9778	0.7680
	0.05	0.1032	0.9646	3.7101	0.0688	0.9681	1.5786	0.0662	0.9654	0.8675
	0.07	0.1241	0.9508	3.2543	0.0866	0.9556	1.6300	0.0789	0.9535	0.9266
	0.09	0.1414	0.9376	2.9292	0.1037	0.9430	1.6348	0.0908	0.9419	0.9631
	0.1	0.1490	0.9312	2.7986	0.1119	0.9367	1.6277	0.0965	0.9361	0.9757
IICA-3	0.01	0.0325	0.9937	4.9549	0.0291	0.9928	1.0114	0.0311	0.9910	0.5726
	0.02	0.0568	0.9864	4.8145	0.0407	0.9865	1.2746	0.0427	0.9842	0.6901
	0.03	0.0756	0.9790	4.3884	0.0505	0.9804	1.4273	0.0516	0.9778	0.7680
	0.05	0.1032	0.9646	3.7101	0.0688	0.9681	1.5786	0.0662	0.9654	0.8675
	0.07	0.1241	0.9508	3.2543	0.0866	0.9556	1.6300	0.0789	0.9535	0.9266
	0.09	0.1414	0.9376	2.9292	0.1037	0.9430	1.6348	0.0908	0.9419	0.9631
	0.1	0.1490	0.9312	2.7986	0.1119	0.9367	1.6277	0.0965	0.9361	0.9757
PSO	0.01	0.0498	0.9921	7.6317	0.0498	0.9901	3.7485	0.0498	0.9877	2.2218
	0.02	0.0702	0.9846	5.7995	0.0702	0.9819	3.2808	0.0702	0.9785	2.0698
	0.03	0.0856	0.9773	4.8928	0.0856	0.9741	2.9850	0.0856	0.9700	1.9594
	0.05	0.1098	0.9632	3.9158	0.1098	0.9592	2.6039	0.1098	0.9542	1.7995
	0.07	0.1290	0.9496	3.3656	0.1290	0.9450	2.3549	0.1290	0.9394	1.6835
	0.09	0.1452	0.9366	2.9989	0.1452	0.9315	2.1730	0.1452	0.9253	1.5926
	0.1	0.1525	0.9302	2.8557	0.1525	0.9250	2.0981	0.1525	0.9186	1.5536
curveFit	0.01	0.0498	0.9921	5.2383	0.0498	0.9901	1.1121	0.0498	0.9877	0.6065
	0.02	0.0702	0.9846	4.8855	0.0702	0.9819	1.3994	0.0702	0.9785	0.7383
	0.03	0.0856	0.9773	4.4129	0.0856	0.9741	1.5505	0.0856	0.9700	0.8240
	0.05	0.1098	0.9632	3.7156	0.1098	0.9591	1.6760	0.1098	0.9542	0.9285
	0.07	0.1290	0.9496	3.2563	0.1290	0.9450	1.7003	0.1290	0.9394	0.9857
	0.09	0.1452	0.9366	2.9301	0.1452	0.9315	1.6846	0.1452	0.9254	1.0176
	0.1	0.1525	0.9302	2.7992	0.1525	0.9250	1.6697	0.1525	0.9186	1.0274

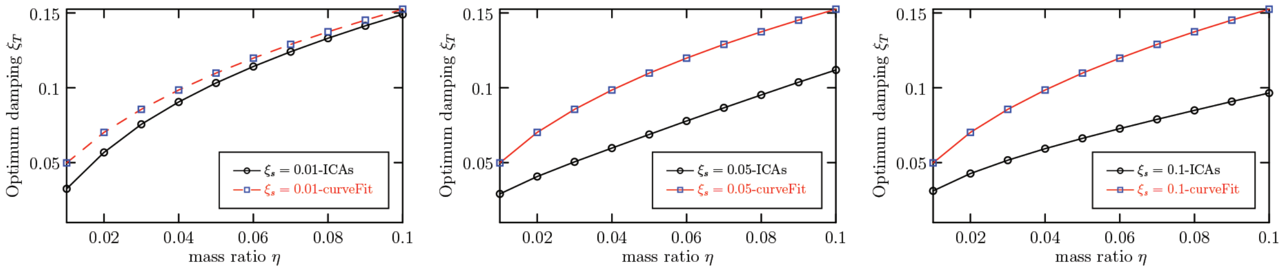

(a) (b) (c)

Figure 5. Optimum damping ξ_T of TMD obtained by ICAs and curve fitting for different ξ_s.

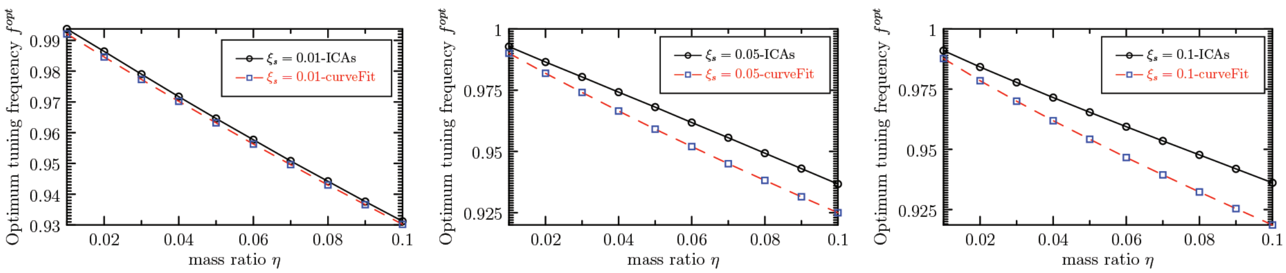

(a) (b) (c)

Figure 6. Optimum tuning frequency f^{opt} of TMD obtained by ICAs and curve fitting for different ξ_s.

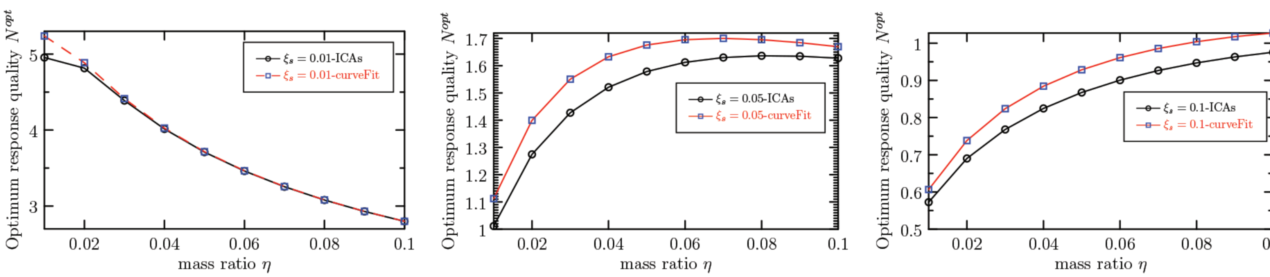

(a) (b) (c)

Figure 7. Optimum response quality N^{opt} of TMD obtained by ICAs and curve fitting for different ξ_s.

3.3. FOPID controller parameter tuning for AVR system

In order to further prove their superiority, the improved ICAs are used to tune the parameters of a FOPID controller for an AVR system. The FOPID controller is an extension of the conventional PID controller using fractional calculus [30]. In a FOPID controller, the orders of the differential and integral terms are noninteger. The transfer function of the FOPID controller is represented as

$$G_c(s) = K_p + \frac{K_i}{s^{\lambda}} + K_d s^{\mu} \quad (\lambda, \mu > 0), \tag{19}$$

where λ, and μ are the orders of the integral and differential terms. Compared with the PID controller, there are two extra parameters in a FOPID controller, which provides more flexibility in controller; therefore, and better control performance can be obtained [30]. Several intelligent optimization methods have been used to design FOPID controllers for AVR systems [31–33]. In this section, the improved ICAs are used to design a FOPID controller for an AVR system. An AVR system equipped with a FOPID controller is shown in Figure 8.

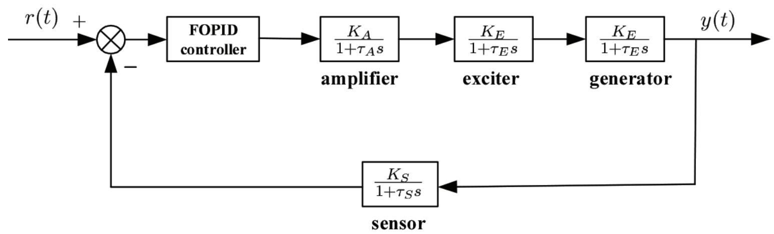

Figure 8. The block diagram of an AVR system with FOPID controller.

Table 6. Optimal values of FOPID controller parameter and corresponding performance indexes obtained by ICA, IICA-1, IICA-2, and IICA-3.

	K_p	K_i	K_d	λ	μ	M_p	E_{ss}	t_r	t_s
ICA	1.2474	0.5973	0.3411	0.9460	1.1487	0.0089	0.0062	0.1666	0.2123
IICA-1	1.3231	0.4392	0.3147	1.0950	1.1444	0.0077	0.0017	0.1761	0.2264
IICA-2	1.0583	0.5183	0.3104	1.0252	1.1021	0	0.0008	0.194	0.2581
IICA-3	0.9742	0.4844	0.2671	1.0323	1.0894	0	0	0.2232	0.3011

To tune the parameters of the FOPID controller, the following performance index is adopted:

$$J(K_p, K_i, K_d, \lambda, \mu) = (1 - e^{-\nu})(M_p + E_{ss}) + e^{-\nu}(t_s - t_r), \tag{20}$$

where M_p is the overshoot of system response, E_{ss} is the steady error, t_s is the settling time, t_r is the raising time, and ν is the weight factor. Similarly, all the algorithms independently run 30 times. The optimal parameter values of the FOPID controller and the values of performance indexes M_p, E_{ss}, t_r, and t_s are listed in Table 6. Figure 9 shows the terminal voltage response of the AVR system with FOPID controller optimized by ICA, IICA-1, IICA-2, and IICA-3. It can be seen from Figure 9 that the FOPID controllers obtained by ICA, IICA-1, and IICA-2 have similar control performance, i.e. the system has faster response speed, oscillates a bit, and has a little steady error. For the FOPID controller obtained by IICA-3, although the system responses are slower than those of ICA, IICA-1, and IICA-2, it oscillates less and has no steady error. This shows that the IICA-3 algorithm performs better than the other reference algorithms.

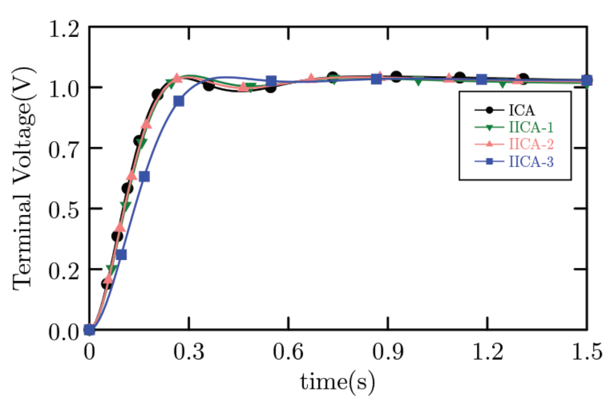

Figure 9. AVR system controlled by FOPID controllers.

4. Conclusion

In this paper, a novel improved imperialist competitive algorithm is presented for global optimization. The ICA is an optimization method based on a sociopolitically motivated strategy. In order to achieve more accurate results with faster speed, two improved schemes for the ICA are proposed. First, a new possession probability in imperialistic competition is proposed by taking the distance between the imperialists and the colony into account. Second, a wavelet mutation operator is added to the ICA to enhance the exploration ability of the ICA. The improved algorithms are tested on six benchmark functions and used to design the optimum parameter of TMD and tune the parameters of a fractional PID controller of an AVR system. Experimental results show that the improved ICAs perform better than the ICA in terms of solution quality and convergence speed, especially in solving multimodal optimization problems.

Acknowledgment

This work was supported by the National Natural Science Foundation of China (Grant No. 61603211).

References

[1] Lin C, Prasad M, Saxena A. An improved polynomial neural network classifier using real-coded genetic algorithm. IEEE T Syst Man Cy A 2015; 45: 1389-1401.

[2] Kennedy J, Eberhart R. Particle swarm optimization. In: Proceedings of IEEE International Conference on Neural Networks; Perth, Australia. Piscataway, NJ, USA: IEEE; 1995. pp. 1942–1948

[3] Dorigo M, Maniezzo V, Colorni A. Ant system: optimization by a colony of cooperating agents. IEEE T Syst Man CY B 1996; 26: 29-41.

[4] Gozde H, Taplamacioglu MC. Comparative performance analysis of artificial bee colony algorithm for automatic voltage regulator (AVR) system. J Franklin Inst 2011; 348: 1927-1946.

[5] Atashpaz-Gargari E, Lucas C. Imperialist competitive algorithm: an algorithm for optimization inspired by imperialistic competition. In: 2007 IEEE Congress on Evolutionary Computation; Singapore. New York, NY, USA: IEEE; 2007. pp. 4661-4667

[6] Abd-Elazim SM, Ali ES. Power system stability enhancement via bacteria foraging optimization algorithm. Arabian J Sci Eng 2013; 38: 599-611.

[7] Abd-Elazim SM, Ali ES. Imperialist competitive algorithm for optimal statcom design in a multimachine power system. Int J Elec Power 2016; 76: 136-146.

[8] Moradifar A, Akbari Foroud A, Gorgani Firouzjah K. Comprehensive identification of multiple harmonic sources using fuzzy logic and adjusted probabilistic neural network. Neural Comput Appl 2017; 3: 1-14.

[9] Mortazavi A, Khamseh AA, Naderi B. A novel chaotic imperialist competitive algorithm for production and air transportation scheduling problems. Neural Comput Appl 2015; 26: 1709-1723.

[10] Zandieh M, Khatami A, Rahmati SHA. Flexible job shop scheduling under condition-based maintenance: improved version of imperialist competitive algorithm. Appl Soft Comput 2017; 58: 449-464.

[11] Mikaeil R, Haghshenas SS, Haghshenas SS, Ataei M. Performance prediction of circular saw machine using imperialist competitive algorithm and fuzzy clustering technique. Neural Comput Appl 2018; 29: 283–292.

[12] Hosseini S, Khaled AA, Vadlamani S. Hybrid imperialist competitive algorithm, variable neighborhood search, and simulated annealing for dynamic facility layout problem. Neural Comput Appl 2014; 25: 1871-1885.

[13] Abdechiri M, Faez K, Bahrami H. Adaptive imperialist competitive algorithm (AICA). In: 9th IEEE International Conference on Cognitive Informatics; 7–9 July 2010; Beijing, China. New York, NY, USA: IEEE. pp. 940-945.

[14] Niknam T, Taherian Fard E, Pourjafarian N, Rousta A. An efficient hybrid algorithm based on modified imperialist competitive algorithm and K-means for data clustering. Eng Appl Artif Intel 2011; 24: 306-317.

[15] Talatahari S, Azar BF, Sheikholeslami R, Gandomi AH. Imperialist competitive algorithm combined with chaos for global optimization. Commun Nonlinear Sci 2012; 17: 1312-1319.

[16] Niknam T, Taherian Fard E, Ehrampoosh S, Rousta A. A new hybrid imperialist competitive algorithm on data clustering. Sādhanā 2011; 36: 293-315.

[17] Goldansaz SM, Jolai F, Anaraki AHZ. A hybrid imperialist competitive algorithm for minimizing makespan in a multi-processor open shop. Appl Math Model 2013; 37: 9603-9616.

[18] Bahrami H, Faez K, Abdechiri M. Imperialist competitive algorithm using chaos theory for optimization (CICA). In: International Conference on Computer Modelling and Simulation; Cambridge, UK. New York, NY, USA: IEEE; 2010. pp. 98-103.

[19] Abdechiri M, Faez K, Bahrami H. Neural network learning based on chaotic imperialist competitive algorithm. In: 2nd International Workshop on Intelligent Systems and Applications; Wuhan, China. New York, NY, USA: IEEE; 2010. pp. 1-5

[20] Coelho LDS, Afonso LD, Alotto P. A modified imperialist competitive algorithm for optimization in electromagnetics. IEEE T Magn 2012; 48: 579-582.

[21] Afonso LD, Mariani VC, Coelho LDS. Modified imperialist competitive algorithm based on attraction and repulsion concepts for reliability-redundancy optimization. Expert Syst Appl 2013; 40: 3794-3802.

[22] Yang S, Yi Y, Shan Z. Gbest-guided imperialist competitive algorithm for global numerical optimization. In: International Conference on Computer Distributed Control and Intelligent Environmental Monitoring; Hunan, China. New York, NY, USA: IEEE; 2012. pp. 352-355.

[23] Idoumghar L, Rin N, Siarry P, Roche R, Miraoui A. Hybrid ICA-PSO algorithm for continuous optimization. Appl Math Comput 2013; 219: 11149-11170.

[24] Khaled AA, Hosseini S. Fuzzy adaptive imperialist competitive algorithm for global optimization. Neural Comput Appl 2015; 26: 813-825.

[25] Ling SH, Iu HH, Chan KY, Lam HK, Yeung BC, Leung FH. Hybrid particle swarm optimization with wavelet mutation and its industrial applications. IEEE T Syst Man CY B 2008; 38: 743-763.

[26] Hermann F. Device for Damping Vibrations of Bodies. US Patent 0989958. 1909.

[27] Leung AYT, Zhang H. Particle swarm optimization of tuned mass dampers. Eng Struct 2009; 31: 715-728.

[28] Bekdaş G, Nigdeli SM. Metaheuristic based optimization of tuned mass dampers under earthquake excitation by considering soil-structure interaction. Soil Dyn Earthq Eng 2017; 92: 443-461.

[29] Bakre SV, Jangid RS. Optimum parameters of tuned mass damper for damped main system. Struct Control Hlth 2007; 14: 448–470.

[30] Podlubny I. Fractional-order systems and $PI^{\lambda}D^{\mu}$-controllers. IEEE T Automat Contr 1999; 44: 208-214.

[31] Zamani M, Sadati N, Ghartemani MK. Design of an H_{∞} PID controller using particle swarm optimization. Int J Control Autom Syst 2009; 7: 273-280.

[32] Biswas A, Das S, Abraham A, Dasgupta S. Design of fractional-order $\mathrm{PI}^{\lambda}\mathrm{D}^{\mu}$ controllers with an improved differential evolution. Eng Appl Artif Intel 2009; 22: 343-350.

[33] Lee CH, Chang FK. Fractional-order PID controller optimization via improved electromagnetism-like algorithm. Expert Syst Appl 2010; 37: 8871-8878.